



## Evaluation of Mathematical Models for Tankers' Maneuvering Motions

Erhan AKSU<sup>1</sup>, Ercan KÖSE<sup>1</sup>

<sup>1</sup>Karadeniz Technical University, Sürmene Faculty of Marine Sciences, [eaksu@ktu.edu.tr](mailto:eaksu@ktu.edu.tr); [ekose@ktu.edu.tr](mailto:ekose@ktu.edu.tr)

### Abstract

In this study, the maneuvering performance of two tanker ships, KVLCC1 and KVLCC2 which have different stern forms are predicted using a system-based method. Two different 3 DOF (degrees of freedom) mathematical models based on the MMG (Maneuvering Modeling Group) concept are applied with the difference in representing lateral force and yawing moment by second and third order polynomials respectively. Hydrodynamic coefficients and related parameters used in the mathematical models of the same scale models of KVLCC1 and KVLCC2 ships are estimated by using experimental data of NMRI (National Maritime Research Institute). The simulations of turning circle with rudder angle  $\pm 35^\circ$ , zigzag ( $\pm 10^\circ/\pm 10^\circ$ ) and zigzag ( $\pm 20^\circ/\pm 20^\circ$ ) maneuvers are carried out and compared with free running model test data of MARIN (Maritime Research Institute Netherlands) in this study. As a result of the analysis, it can be summarised that MMG model based on the third order polynomial is superior to the one based on the second order polynomial in view of estimation accuracy of lateral hull force and yawing moment.

**Keywords:** Ship Maneuvering, MMG Model, Tankers.

### Tankerlerin Manevra Hareketleri için Matematiksel Modellerin Değerlendirilmesi

#### Öz

Bu çalışmada farklı kış formlarına sahip olan KVLCC1 ve KVLCC2 iki tanker gemisinin manevra performansları sistem temelli metoda dayalı olarak tahmin edilmiştir. Yanal kuvvetin ve savrulma momentinin ikinci ve üçüncü derece polinomlarla yazılması suretiyle, MMG (Matematiksel Modelleme Grubu) konseptine dayalı iki farklı 3 DOF (serbestlik dereceli) matematiksel model uygulanmıştır. Matematiksel modellerdeki KVLCC1 ve KVLCC2 gemilerinin aynı ölçekte modellerinin hidrodinamik katsayıları ve ilgili parametreleri NMRI'nin (Ulusal Denizcilik Araştırma Enstitüsü, Japonya) deneysel verileri kullanılarak tahmin edilmiştir. Bu çalışmada dümen açısı  $\pm 35^\circ$  ile dönme, zigzag ( $\pm 10^\circ/\pm 10^\circ$ ) ve zigzag ( $\pm 20^\circ/\pm 20^\circ$ ) manevra simülasyonları MARIN'nin (Hollanda Denizcilik Araştırma Enstitüsü) serbest model deney verileri ile birlikte yer almış ve karşılaştırılmıştır. Analizler sonucunda, yanal tekne kuvveti ve savrulma momentinin doğruluğu açısından üçüncü derece polinomla ifade edilmiş MMG modelinin ikinci derece ile ifade edilen modele göre daha üstün olduğu görülmektedir.

**Anahtar Kelimeler:** Gemi Manevra, MMG Modeli, Tankerler.

## 1. Introduction

A design requirement for all marine vehicles is adequate maneuvering ability. Ship's maneuverability is the ability of a ship to keep or change its state of motion under the control actions (i.e. tugboats in the harbor maneuvers [1]). There are different ways for the prediction of a ship's maneuverability, i.e. predictions based on free running model tests, predictions based on captive model tests, predictions based on empirical methods, predictions based on system identification methods, predictions using viscous flow CFD (Computational Fluid Dynamics) (using RANS (Reynolds Reynolds Averaged Navier-Stokes) codes) and predictions using potential flow CFD (using panel codes, vortex lattice and vortex blob codes) [2]. Captive model tests are conducted with a scale ship model in towing tanks where the model is forced to move in a prescribed manner. These tests are conducted to determine the hydrodynamic coefficients in the corresponding mathematical models. Generally speaking, there are two distinct groups of mathematical models for ship maneuvering motion simulations according to the manner to express the hydrodynamic forces and moments acting on the vessel. One of them is the so called MMG model proposed by the Maneuvering Modeling Group in Japanese Towing Tank Conference [3]. Many applications based on MMG mathematical model are available in the literature [4, 6]. In the MMG mathematical models, hydrodynamic forces acting on the whole ship are decomposed into individual parts of hull, propeller and rudder respectively, while the interactions between these parts are taken into account by a series of coefficients. Compared to the other group of mathematical models, the formal models, an MMG model has a relative more clear physical explanation for each term contained in the model and is constructed as simple as possible. Furthermore;

the structural form of the model allows external disturbances caused by wind, waves and currents to be easily integrated into the maneuvering model. Inoue studied hydrodynamic coefficients in the case of maneuvering motions and suggested the approximation formulae for estimation of lateral force and moment [7, 8]. In Simman 2008 workshop, studies had been carried out for the prediction of ship maneuvering motions for three different hull forms which are tanker (KVLCC1-KVLCC2), container ship (KCS), and surface combatant (DTMB 5415) [9]. In this workshop, different ship maneuvering prediction methods were used. In the study using MMG model, hull forces and moment were considered as the function of drift angle and yaw rate. The lateral hull force and yawing moment were expressed by the third order polynomial for KVLCC1, KVLCC2 and KCS hulls [10]. Also hydrodynamic coefficients and rudder, rudder horn and propeller effects were studied under different conditions for KVLCC1 and KVLCC2 hulls [11]. Similar studies were presented in the research report [12]. Recently, the MMG standard method was summarised by Yasukawa [13] and an application was made using experimental data for KVLCC2 hull. Here, lateral force and yawing moment were represented by third order polynomials.

In this study, two tanker hull forms having different stern sections are examined for the prediction of maneuvering motions. In this regard, all hydrodynamic coefficients and parameters in the MMG model have been calculated from the experimental data where the lateral hull force and yawing moment are expressed by second order and third order polynomials. Finally, simulations are carried out and compared with free running model test data in turning circle and zigzag maneuvering motions.

## 2. Description of Hulls

Two tanker ship forms are examined

here and one of them has barge type stern frame-lines with a fine stern end bulb i.e. relatively V-shaped frame-lines (KVLCC1) while the other one has more U-shaped stern frame-lines (KVLCC2). Figure 1 shows the KVLCC1 and KVLCC2 body plans and full scale. Additionally, the model dimensions of these tankers are given in Table 1[14].

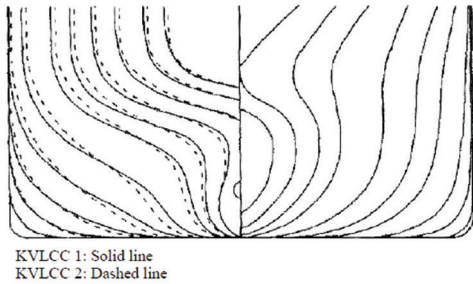


Figure 1. Hull Forms of KVLCC1 and KVLCC2 [14]

### 3. Mathematical Model

A 3DOF model based on the MMG mathematical model is implemented in the simulations of ship maneuvering motions. As can be seen in Figure 2, the origin of the ship-fixed reference frame is located at the mid-ship position and equations of motion are written as follows:

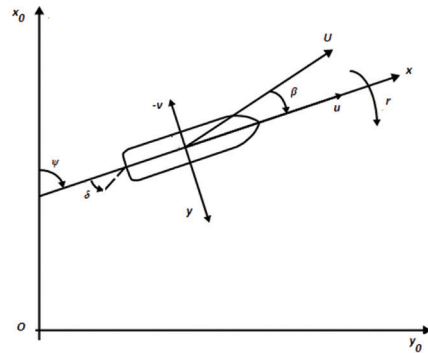


Figure 2. The Body-fixed Coordinate Systems

Table 1. Dimensions of Hulls, Rudders and Propellers [14]

	KVLCC1			KVLCC2		
	Full Scale	NMRI	MARIN	Full scale	NMRI	MARIN
Scale	1.000	110.000	45.714	1.000	110.000	45.714
Main particulars						
Lpp (m)	320.0	2.9091	7.0000	320.0	2.9091	7.0000
Bwl (m)	58.0	0.5273	1.2688	58.0	0.5273	1.2688
T (m)	20.8	0.1891	0.4550	20.8	0.1891	0.4550
Displacement (m <sup>3</sup> )	312738	0.2350	3.2737	312738	0.2349	3.2724
CB	0.8101	0.8101	0.8101	0.8098	0.8098	0.8098
LCG (m)	11.1	0.1009	0.244	11.1	0.1009	0.244
Rudder						
S (mov. part) (m <sup>2</sup> )	112.264	0.009278	0.05372	112.264	0.009278	0.05372
λ (aspect ratio)	1.826	1.826	1.826	1.826	1.826	1.826
Turn rate (deg/s)	2.34	24.5	15.8	2.34	24.5	15.8
Propeller						
D <sub>p</sub> (m)	9.86	0.0896	0.204	9.86	0.0896	0.204
η (D <sub>p</sub> /R <sub>H</sub> )	0.6237	0.6237	0.6237	0.6237	0.6237	0.6237

./..

**Table 1.** Dimensions of Hulls, Rudders and Propellers [14] (Cont’)

Service speed						
U (m/s, full scale: kn)	15.5	0.760	1.179	15.5	0.760	1.179
Fn	0.142	0.142	0.142	0.142	0.142	0.142

$$\begin{aligned}
 m(\dot{u} - vr - x_G r^2) &= X \\
 m(\dot{v} + ur + x_G \dot{r}) &= Y \quad (1)
 \end{aligned}$$

$$I_{ZZ} \dot{r} + mx_G(\dot{v} + ur) = N$$

In Figure 2, equations of motion, respectively X, Y, N denote longitudinal force, lateral force, and yawing moment;  $\dot{u}, \dot{v}, \dot{r}$  denote the surge acceleration, sway acceleration, and yaw acceleration;  $u, v,$  and  $r$  denote the surge velocity, sway velocity, and yaw rate in the ship-fixed reference frame. Besides,  $m$  is the mass of ship;  $I_{ZZ}$  is the moment of inertia about z axis;  $x_G$  is the longitudinal location of the ship’s gravity center from mid-ship position;  $U(= \sqrt{u^2 + v^2})$  is the total velocity;  $\beta = \tan^{-1}(-v/u)$  is the drift angle;  $\psi$  is heading angle; and  $\delta$  is rudder angle.

In the basic structure of the MMG model, the representation of the forces and moment in the horizontal plane are decomposed as follows [6]:

$$\begin{aligned}
 X &= X_H + X_P + X_R \\
 Y &= Y_H + Y_P + Y_R \quad (2)
 \end{aligned}$$

$$N = N_H + N_P + N_R$$

The terms with subscripts H, P and R refer to different contributions from the hull, propeller and rudder.

### 3.1. Hull Forces and Moment

Hull forces and moment consist of acceleration and velocity dependent contributions. Since CMT experimental test fail to find added masses and added inertia moment, corresponding coefficients can be estimated using proper empirical

formula[15].

Hydrodynamic force acting on the hull in the x-direction is described as follows:

$$X_H = -m_x \dot{u} + X_0 + X_{vv} v^2 + (X_{vr} + m_y)vr + X_{rr} r^2 + X_{vvvv} v^4 \quad (3)$$

Velocity dependent force and moment of lateral force and yawing moment on the hull can also be decomposed into linear and nonlinear terms. In general, second or third order polynomial is chosen for non-linear terms [16]. In the current analysis, for Simulation A-C, third order polynomials (Eqs.4,5) are preferred while second order polynomial (Eqs. 6,7) is chosen for Simulation B-D.

Model 1 (for Simulation A-C):

$$Y_H = -m_y \dot{v} + Y_v v + (Y_r - m_x u)r + Y_{vvv} v^3 + Y_{rrr} r^3 + Y_{vvv} v^2 r + Y_{vrr} vr^2 \quad (4)$$

$$N_H = -J_{zz} \dot{r} + N_v v + N_r r + N_{vvv} v^3 + N_{rrr} r^3 + N_{vvv} v^2 r + N_{vrr} vr^2 \quad (5)$$

Model 2 (for Simulation B-D):

$$N_H = -m_y \dot{v} + Y_v v + (Y_r - m_x u)r + Y_{|v|} |v| + Y_{|v|r} |v|r + Y_{|r|} |r| + Y_{|v|r} |r|v + Y_{|r|} |r|r \quad (6)$$

$$N_H = -J_{zz} \dot{r} + N_v v + N_r r + N_{|v|} |v| + N_{|v|r} |v|r + N_{|r|} |r| + N_{|r|} |r|r \quad (7)$$

### 3.2. Propeller Force

Hydrodynamic forces and moment due to the propeller can be written as follows:

$$X_P = (1 - t_p)T_P = (1 - t_p)\rho n^2 D_P^4 K_T(J_P)$$

$$Y_P = 0 \quad (8)$$

$$N_P = 0$$

where

$$K_T(J_P) = a_0 + a_1 J_P + a_2 J_P^2 \quad (9)$$

$$J_P = u(1 - w_p)/(nD_P) \quad (10)$$

In these expressions,  $t_p$  is thrust deduction factor;  $T_p$  is propeller thrust which is the force that allows the ships to move;  $K_T(J_p)$  is open water characteristic of the propeller which is assumed to be the second order polynomial function of  $J_p$ ;  $J_p$  is advance coefficient;  $n$  is revolutions per second of propeller;  $w_p$  is wake coefficient at propeller; and  $D_p$  is diameter of propeller.

### 3.3. Rudder Force

Hydrodynamic forces and moment due to rudder can be expressed in terms of rudder normal force as follows:

$$\begin{aligned} X_R &= -(1 - t_R)F_N \sin\delta \\ Y_R &= -(1 + a_H)F_N \cos\delta \\ N_R &= -(x_R + a_H x_H)F_N \cos\delta \end{aligned} \tag{11}$$

In the above equations,  $t_R$ ,  $a_H$ ,  $x_H$  are interaction coefficients between hull and rudder;  $x_R$  is longitudinal coordinate of rudder position which is -0.5 L and rudder angle  $\delta$  is positive for deflection to starboard. Rudder normal force  $F_N$  for the rudder is defined as follows:

$$F_N = \frac{1}{2} \rho f_a A_R U_R^2 \sin\alpha_R \tag{12}$$

$$f_a = 6.13\lambda / (\lambda + 2.25) \tag{13}$$

$$U_R = \sqrt{u_R^2 + v_R^2} \tag{14}$$

$$u_R = \varepsilon(1 - w_p) \sqrt{\eta \left\{ 1 + k \left( \sqrt{1 + \frac{8K_T}{\pi J_p^2}} - 1 \right) \right\}^2 + (1 - \eta)} \tag{15}$$

$$v_R = U \gamma_R \beta_R = U \gamma_R (\beta - l_R' r') \tag{16}$$

$$\alpha_R = \delta - \text{Arctan}(v_R/u_R) \cong \delta - v_R/u_R \tag{17}$$

In these expressions,  $A_R$  is profile area of movable part of rudder;  $f_a$  is gradient of the normal force coefficient which can be estimated using Fujii's formula[17];  $\lambda$  is aspect ratio of rudder which is calculated by movable part of rudder and rudder

height;  $u_R$  and  $v_R$  are longitudinal and lateral component of the effective inflow velocity at the rudder;  $\varepsilon$  is ratio of wake fraction at propeller and rudder;  $k$  is experimental constant for expressing  $u_R$ ;  $\eta$  is ratio of propeller diameter to rudder height;  $\gamma_R$  is a coefficient for flow straightening;  $l_R'$  is effective longitudinal position of rudder;  $\beta_R$  is the effective inflow angle to the rudder in maneuvering motions; and  $\alpha_R$  is the effective inflow angle to the rudder.

### 4. Extraction of Hydrodynamic Coefficients and Parameters

One of the methods used to determine the hydrodynamic coefficients and related parameters is to perform a series of experimental studies on a specific scale model of the full scale ship. In this section, experiments of 1/110 scaled KVLCC1 and KVLCC2 models belonging to NMRI in the Simman 2008 workshop were discussed[18]. These are resistance test, self-propulsion test, open water test of propeller, rudder test, oblique towing test, and circular motion test. For related tests, the speed of the model was 0.76 [m/s], which corresponds to the speed of the full scale ship (15.5 [knot]). As seen in Table 2, the related terms were derived from different experimental types.

Table 2. Test Types for Related Parameters

Test Type	Related Parameters
Open Water Propeller	$K_T (a_{0p}, a_{1p}, a_{2p})$
Resistance	$X_{0'}$
Self Propulsion Test	$(1-t_p), (1-w_p)$
Static Rudder Test	$(1-t_R), a_{Hr}, x_{Hr}, \varepsilon, k$
Circular Motion Test	$X_{vv}', X_{vr}', X_{rr}', X_{vvv}'$ $Y_v', Y_r', Y_{vv}', Y_{vr}', Y_{rr}', Y_{vvr}'$ $Y_{v v}', Y_{v r}', Y_{r v}', Y_{r r}'$ $N_v', N_r', N_{vv}', N_{vr}', N_{rr}', N_{vvr}'$ $N_{ v v}', N_{ v r}', N_{ r v}', N_{ r r}'$ $Y_{R'} l_{R'}$

The parameters of the open water characteristic of the propeller ( $a_0, a_1, a_2$ ) shown in Figure 3 are calculated by fitting a second order polynomial to the data obtained from the open water propeller test. In order to calculate  $X_{\rho'}$  as shown in Figure 4, the longitudinal force magnitude corresponding to the service speed is taken into consideration for the hull with rudder attachment at four different speeds in the resistance test. The thrust deduction factor  $t_p$ , wake coefficient  $w_p$  and revolutions per second of propeller  $n$  were determined by using the self propulsion test in Figure 5.

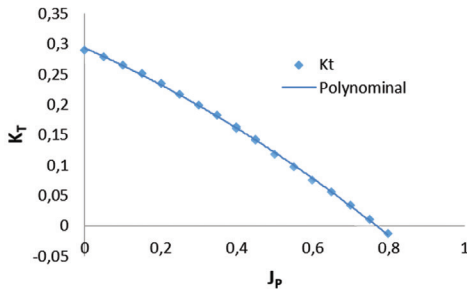


Figure 3. Open Water Propeller Test for KVLCC1 Model

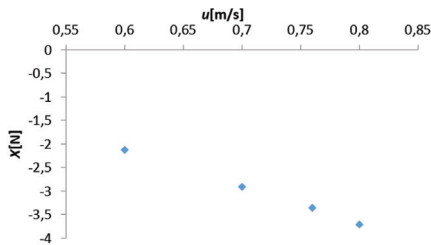


Figure 4. Resistance Test for KVLCC1 Model

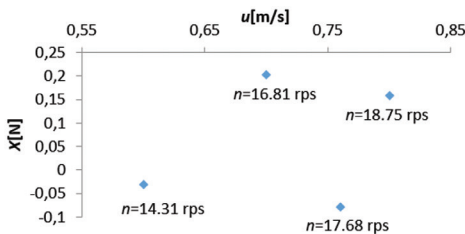


Figure 5. Self-propulsion Test for KVLCC1 Model

In the static rudder test, the rudder is held at different angles while the hull is moving linearly. Also, in this experiment, three different loading ( $J_s = u/nD_p$ ;  $n$  was changed) were applied on the propeller. In the static rudder test, the lateral and radial velocities of the hull are zero because of the linear motion of the hull ( $v=r=0$ ). As a result, the rudder forces and moment are expressed as follows:

$$\begin{aligned} X - X_0 - (1 - t_p)T_p &= X_R = -(1 - t_R)F_N \sin \delta \\ Y &= Y_R = -(1 + a_H)F_N \cos \delta \\ N &= N_R = -(x_R + a_H x_H)F_N \cos \delta \end{aligned} \tag{18}$$

From the above equations, hull-rudder interaction coefficients ( $t_R, a_H, x_H$ ) are calculated by the curve to be fitted to the

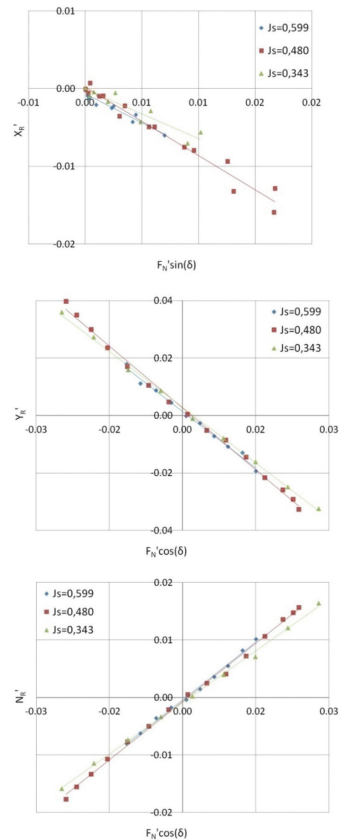


Figure 6. Estimation for Interaction Coefficients for KVLCC1 Model



relationship between rudder forces and moment ( $X_{R'} Y_{R'} N_{R'}$ ) and rudder normal force  $F_N$  multiplied by  $\cos\delta$  (or  $\sin\delta$ ) as seen in Figure 6. For interaction coefficients the model self propulsion point was selected as the propeller loading point.

Another parameter lateral effective inflow velocity at the rudder equals zero in the same experiment ( $v_R = 0$ ). As a result, the normal force of the rudder in Eqs. 12 is written as follows:

$$F_N = \frac{1}{2} \rho f_a A_R u_R^2 \sin\delta \quad (19)$$

The longitudinal effective inflow velocity at the rudder  $u_R$  is calculated with the help of the measured rudder normal force. In addition, the open water characteristic of the propeller  $K_T(J_p)$ , the advance coefficient  $J_p$  and the flow velocity in the propeller  $u_p (= u(1-w_p))$  in Eqs. 15 are calculated at each propeller loading. Thus,  $\varepsilon$  and  $k$  are calculated from the relationship between  $u_R/u_p$  and  $\sqrt{1 + 8K_T/\pi J_p^2} - 1$  and given in Figure 7.

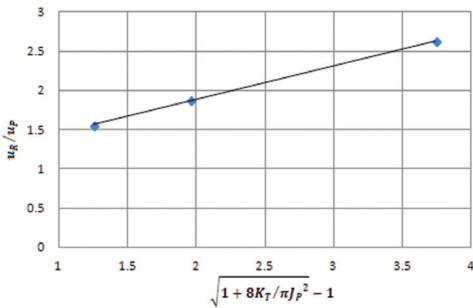


Figure 7. Relation Between  $u_R/u_p$  and  $\sqrt{1 + 8K_T/\pi J_p^2} - 1$

Hydrodynamic coefficients of hull forces and moment ( $X_{v'} X_{vr'} Y_{v'} Y_{vr'} N_{v'} N_{vr}'$ , ....etc.) are obtained by circular motion test results and these tests were done at different sway velocities and yaw rates, while rudder angle is zero and the model runs at ship self-propulsion point. With the help of interaction coefficients calculated here,

lateral and yaw rate dependent variation of total hull force and moment is obtained by subtracting the propeller and rudder force and moment from the total force and moment. As a result, the hull forces and moment are expressed as follows:

$$\begin{aligned} X_H &= X - (1 - t_p)T_p \\ Y_H &= Y + (1 + a_H)F_N \quad (20) \\ N_H &= N + (x_R + a_H x_H)F_N \end{aligned}$$

Figure 8 shows the surfaces which are fitted to the nodal values of the forces and moments. Coefficients of the two variables polynomial that define the surface correspond to hydrodynamic coefficients of mathematical models. Thus, the hydrodynamic coefficients of hull forces and moment are calculated.

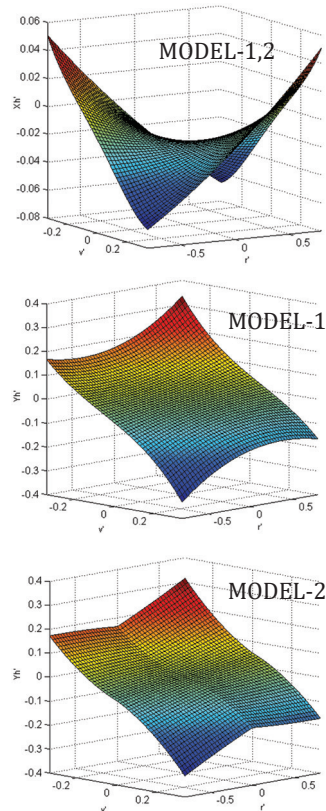
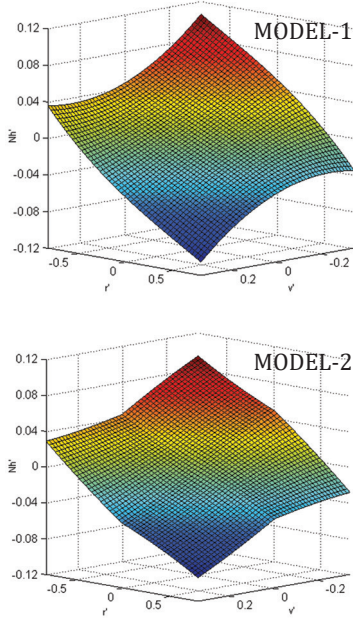


Figure 8. Relationship Between Lateral Velocity and Yaw Rate of Hull Forces and Moment of KVLCC1 Model



**Figure 8.** Relationship Between Lateral Velocity and Yaw Rate of Hull Forces and Moment of KVLCC1 Model (Cont')

For the calculation of coefficient for flow straightening  $\gamma_R$  and effective longitudinal coordinate of rudder  $l'_R$ , which are calculated from the condition that the rudder normal force is zero, again using the CMT data. The rudder normal force is dimensionless and is obtained as follows [13]:

$$F_N' = \frac{A_R f_a}{Ld} (u_R'^2 + v_R'^2) \sin(\delta - v_R'/u_R') \quad (21)$$

If a derivative is derived from Eqs. 21 in terms of  $\delta$ , the following equation is obtained:

$$\frac{dF_N'}{d\delta} = \frac{A_R f_a}{Ld} (u_R'^2 + v_R'^2) \cos(\delta - v_R'/u_R') \quad (22)$$

From the equation of zero normal force condition,  $\delta_{FNO} = v_R'/u_R'$  equals to Eqs. 22 as follows:

$$\left. \frac{dF_N'}{d\delta} \right|_{\delta=\delta_{FNO}} = \frac{A_R f_a}{Ld} u_R'^2 (1 + \delta_{FNO}^2) \quad (23)$$

As a result, for the component in the longitudinal direction of the flow velocity in the rudder, the following formula is obtained:

$$u_R' = \sqrt{\left. \frac{dF_N'}{d\delta} \right|_{\delta=\delta_{FNO}} \frac{Ld}{A_R f_a} \frac{1}{(1 + \delta_{FNO}^2)}} \quad (24)$$

$u_R'$  is calculated from the  $\delta_{FNO}$  and  $dF_N'/d\delta$  magnitudes obtained from experiments. Thus, the component in the lateral direction of the flow velocity in the rudder  $v_R'$  is calculated from  $v_R' = u_R' \delta_{FNO}$ . Utilizing Eqs. 16, as shown in Figure 9,  $\gamma_R$  and  $l'_R$  are computed with the aid of curve fitting in relation to  $\beta_R - v_R'$ .

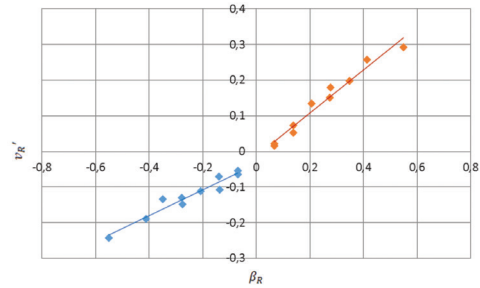


**Figure 9.** Relationship Between  $\beta_R - v_R'$  of KVLCC1 Model

Two sets of simulations have been carried out there. Simulations A and C are performed based on Model 1 while simulations B and D are performed based on Model 2. Both ship forms were simulated in each set; KVLCC1 was examined in simulations A and B while KVLCC2 was examined in simulations C and D. For KVLCC1 and KVLCC2 models, all parameters in each mathematical model are given in Tables 3,4,5,6.

**Table 3.** Parameters for Propeller Force

	Simulation A-B (KVLCC1)	Simulation C-D (KVLCC2)
$n$ (rps)	17.69	17.93
$1 - t_p$	0.811	0.768
$1 - w_p$	0.579	0.543



**Table 4.** Parameters for Rudder Force

	Simulation A-B (KVLCC1)	Simulation C-D (KVLCC2)
$1 - t_R$	0.849	0.811
$a_H$	0.428	0.436
$x_H'$	-0.407	-0.381
$\varepsilon$	1.051	1.12
$k$	0.529	0.495
$\gamma_R (\beta_R < 0)$	0.367	0.397
$\gamma_R (\beta_R > 0)$	0.605	0.643
$l_R'$	-0.687	-0.708

**Table 5.** Hydrodynamic Coefficients for Hull (KVLCC1)

Simulation A		Simulation B	
$X_0'$	-0.0212	$X_0'$	-0.0212
$X_{vv}'$	-0.0742	$X_{vv}'$	-0.0742
$X_{vr}' + m_y'$	0.2154	$X_{vr}' + m_y'$	0.2154
$X_{rr}'$	0.0121	$X_{rr}'$	0.0121
$X_{vvvv}'$	1.0510	$X_{vvvv}'$	1.0510
$Y_v'$	-0.2968	$Y_v'$	-0.1720
$Y_r' - m_x'$	0.0550	$Y_r' - m_x'$	0.0438
$Y_{vvv}'$	-1.6200	$Y_{ v v}'$	-0.8756
$Y_{rrr}'$	0.0091	$Y_{ v r}'$	0.0739
$Y_{vvr}'$	0.3616	$Y_{ r v}'$	-0.2978
$Y_{vrr}'$	-0.3823	$Y_{ r r}'$	0.0232
$N_v'$	-0.1415	$N_v'$	-0.1583
$N_r'$	-0.0490	$N_r'$	-0.0439
$N_{vvv}'$	-0.0025	$N_{ v v}'$	0.0529
$N_{rrr}'$	-0.0111	$N_{ v r}'$	-0.0649
$N_{vvr}'$	-0.2741	$N_{ r v}'$	0.0560
$N_{vrr}'$	0.0612	$N_{ r r}'$	-0.0129

**Table 6.** Hydrodynamic Coefficients for Hull (KVLCC2)

Simulation C		Simulation D	
$X_0'$	-0.0213	$X_0'$	-0.0213
$X_{vv}'$	-0.0473	$X_{vv}'$	-0.0473
$X_{vr}' + m_y'$	0.2241	$X_{vr}' + m_y'$	0.2241

**Table 6.** Hydrodynamic Coefficients for Hull (KVLCC2) (Cont')

$X_{rr}'$	0.0106	$X_{rr}'$	0.0106
$X_{vvvv}'$	0.8206	$X_{vvvv}'$	0.8206
$Y_v'$	-0.3139	$Y_v'$	-0.1886
$Y_r' - m_x'$	0.0607	$Y_r' - m_x'$	0.0510
$Y_{vvv}'$	-1.5890	$Y_{ v v}'$	-0.8705
$Y_{rrr}'$	0.0071	$Y_{ v r}'$	0.0705
$Y_{vvr}'$	0.3652	$Y_{ r v}'$	-0.3105
$Y_{vrr}'$	-0.3915	$Y_{ r r}'$	0.0196
$N_v'$	-0.1371	$N_v'$	-0.1502
$N_r'$	-0.0486	$N_r'$	-0.0422
$N_{vvv}'$	-0.0311	$N_{ v v}'$	0.0329
$N_{rrr}'$	-0.0124	$N_{ v r}'$	-0.0716
$N_{vvr}'$	-0.2903	$N_{ r v}'$	0.0506
$N_{vrr}'$	0.0558	$N_{ r r}'$	-0.0150

In this section, length is non-dimensionalized by  $L$ , linear velocities are non-dimensionalized by  $U$ , angular velocity is non-dimensionalized by  $U/L$ , masses are non-dimensionalized by  $(1/2)\rho L^2 d$ , inertias are non-dimensionalized by  $(1/2)\rho L^4 d$ , forces are non-dimensionalized by  $(1/2)\rho L d U^2$  and moment are non-dimensionalized by  $(1/2)\rho L^2 d U^2$ .

**5. Results and Discussions of Simulations**

Turning circle tests ( $\delta = \pm 35^\circ$ ) and zigzag maneuvering tests ( $\delta = \pm 10^\circ, \delta = \pm 20^\circ$ ) are simulated with the help of the hydrodynamic coefficients and related parameters obtained from the CMT data. Results of the simulations are compared with free running model test results which were obtained in a 1/45.714 scaled model ( $L = 7.000$  m) by MARIN (Maritime Research Institute Netherlands) [18]. In the simulations, initial approach speed is 0.76 m/s and propeller revolution is constant throughout the simulations. Simulation results are given in non-dimensional form to provide comparison.

As shown in Figure 10, the simulation

./..

results of the mathematical models are given for the KVLCC1 hull in terms of turning trajectories, ratio of total velocities to initial total velocities, drift angles and yaw rates for starboard-port turning circle maneuvering motions. Also, advance, tactical diameter, transfer indices and absolute errors are given in Table 7. In general, Simulation A shows better agreement with the free running model test results compared to Simulation B. However; the results of both simulations at portside turning circle tests

not create a problem for small amplitude motion, but, for harsh maneuvering motion, this leads differences between test results and estimation of the trajectories of turning portside and starboard. Because, wake coefficient calculated from self-propulsion test is closed to the coefficient for starboard turning motions. For this reason, the portside turning simulation is not as good as the starboard turning simulation.

Figure 11 and Figure 12 show simulation results of the mathematical models for the

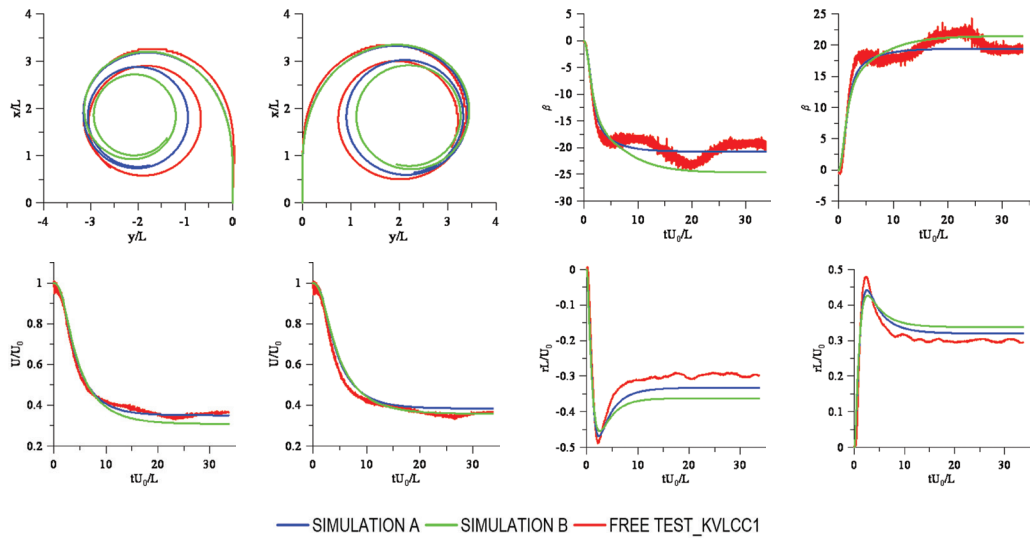


Figure 10. Turning Circle Test of KVLCC1 (Rud. ang:-35° & 35°)

Table 7. Comparison of Turning Indices of KVLCC1 Model

Simulation Type	Indices	Exp.	Sim. A	Sim. B	Absolute Error A	Absolute Error B
Turning circle (stb.)	$A_D'$	3.28	3.26	3.28	0.02	0.00
	$D_T'$	3.28	3.34	3.37	0.06	0.09
	$T_R'$	1.30	1.43	1.48	0.13	0.18
Turning circle (port)	$A_D'$	3.19	3.11	3.13	0.08	0.06
	$D_T'$	3.07	3.08	3.06	0.01	0.01
	$T_R'$	1.17	1.32	1.34	0.15	0.17

diverge from the free running model test results. This can be explained as follows: the wake characteristic of the propeller is not symmetric; therefore, constant acceptance of the wake coefficient does

KVLCC1 in terms of ratio of total velocities to initial total velocities, drift angles, yaw rates as well as heading angles for zigzag ( $\pm 10^\circ/\pm 10^\circ$  and  $\pm 20^\circ/\pm 20^\circ$ ) maneuvering motions. In Table 8, the first overshoot angle

and the second overshoot angle indices and absolute errors are given for KVLCC1 hull. For zigzag ( $\pm 10^\circ/\pm 10^\circ$ ) maneuvering motions, Simulation A gives more accurate results than Simulation B in terms of

overshoot angles in comparison to free running model tests. For zigzag ( $\pm 20^\circ/\pm 20^\circ$ ) maneuvering motions, Simulation A and Simulation B give similar results.

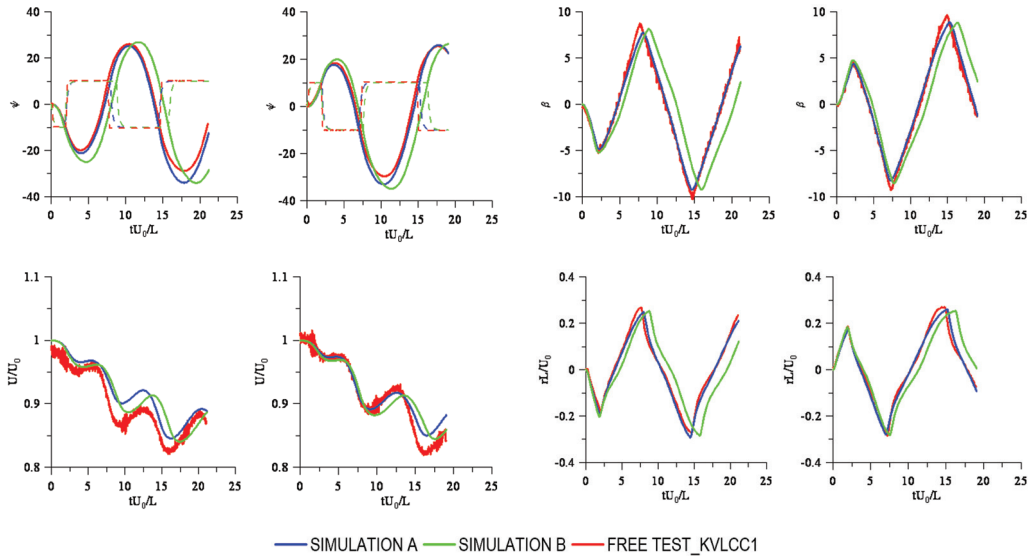


Figure 11. Zigzag Test of KVLCC1 (Rud. ang:  $-10^\circ/10^\circ$  &  $10^\circ/-10^\circ$ )

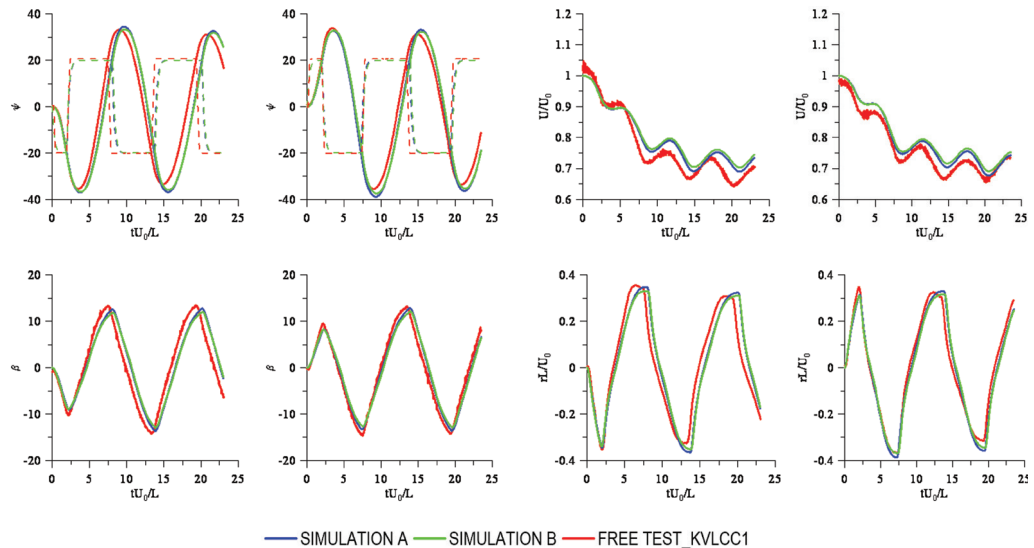


Figure 12. Zigzag Test of KVLCC1 (Rud. ang:  $-20^\circ/20^\circ$  &  $20^\circ/-20^\circ$ )

**Table 8.** Comparison of Zigzag Indices of KVLCC1 Model

Simulation Type	Indices (°)	Exp.	Sim. A	Sim. B	Absolute Error A	Absolute Error B
Zigzag (10°/-10°)	1 <sup>st</sup> OSA	8.4	7.62	9.99	0.78	1.59
	2 <sup>nd</sup> OSA	19.6	23.06	24.98	3.46	5.38
Zigzag (-10°/10°)	1 <sup>st</sup> OSA	10	11.22	14.99	1.22	4.99
	2 <sup>nd</sup> OSA	16.1	15.16	16.89	0.94	0.79
Zigzag (20°/-20°)	1 <sup>st</sup> OSA	13.9	12.72	12.94	1.18	0.96
	2 <sup>nd</sup> OSA	15.5	18.83	17.42	3.33	1.92
Zigzag (-20°/20°)	1 <sup>st</sup> OSA	15.4	16.99	16.73	1.59	1.33
	2 <sup>nd</sup> OSA	13.2	14.9	13.36	1.70	0.16

With similar simulations for the other tanker form which have different stern form, Figure 13. shows it when compared with experimental results of trajectory, speed loss, drift angle and yaw rate parameters for the turning circle test, Simulation C gives more accurate results than Simulation D. A

similar case is observed for the portside turning circle test and the trajectory parameter is diverged from the free running model test results. Advance, tactical diameter, transfer indices and absolute errors are given for KVLCC2 hull in Table 9.

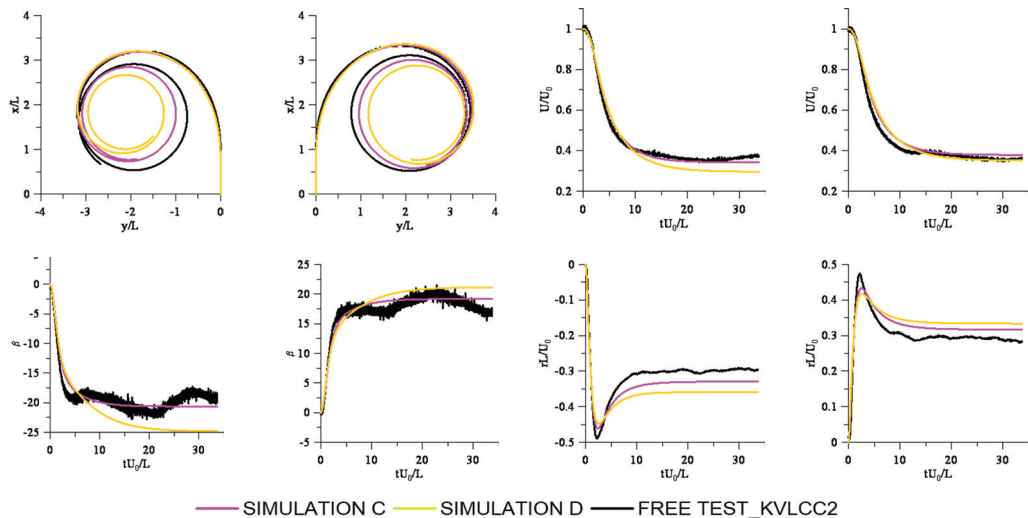


**Figure 13.** Turning Circle Test of KVLCC2 (Rud. ang:-35° & 35°)

**Table 9.** Comparison of Turning Indices of KVLCC2 Model

Simulation Type	Indices	Exp.	Sim. C	Sim. D	Absolute Error C	Absolute Error D
Turning circle (stb.)	A <sub>D</sub> '	3.25	3.27	3.30	0.02	0.05
	D <sub>T</sub> '	3.34	3.40	3.44	0.06	0.10
	T <sub>R</sub> '	1.36	1.47	1.52	0.11	0.16
Turning circle (port)	A <sub>D</sub> '	3.11	3.12	3.14	0.01	0.03
	D <sub>T</sub> '	3.08	3.12	3.10	0.04	0.02
	T <sub>R</sub> '	1.22	1.35	1.38	0.13	0.16

As it can be seen from Figure 14. and Figure 15., for zigzag ( $\pm 10^\circ/\pm 10^\circ$  and  $\pm 20^\circ/\pm 20^\circ$ ) maneuvering motions, simulation results of the same parameters are given. For zigzag ( $\pm 10^\circ/\pm 10^\circ$ ) maneuvering motions, Simulation D gives more accurate results than Simulation C.

Similarly, the results of both simulations are approximately the same for zigzag ( $\pm 20^\circ/\pm 20^\circ$ ) maneuvering motions. In Table 10, the first overshoot angle and second overshoot angle indices and absolute errors are given for KVLCC2 hull.

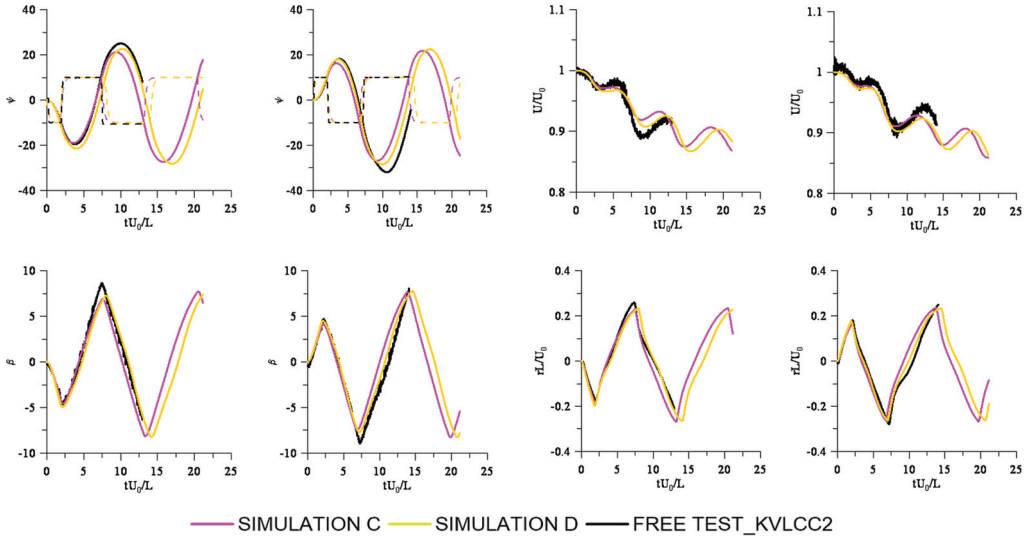


Figure 14. Zigzag Test of KVLCC2 (Rud. ang:  $-10^\circ/10^\circ$  &  $10^\circ/-10^\circ$ )

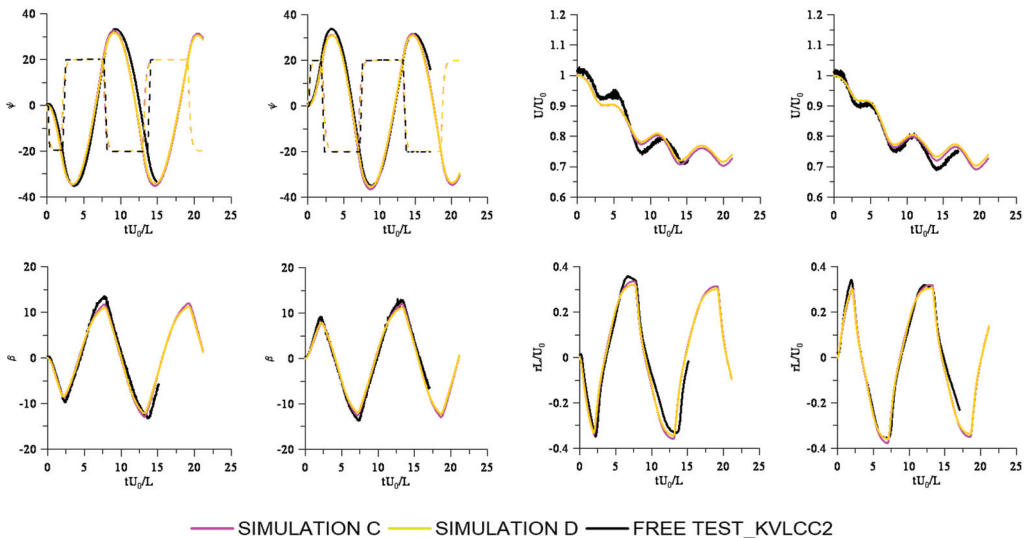


Figure 15. Zigzag Test of KVLCC2 (Rud. ang:  $-20^\circ/20^\circ$  &  $20^\circ/-20^\circ$ )

**Table 10.** Comparison of Zigzag Indices of KVLCC2 Model

Simulation Type	Indices (°)	Exp.	Sim. C	Sim. D	Absolute Error C	Absolute Error D
Zigzag (10°/-10°)	1 <sup>st</sup> OSA	8.2	6.27	7.95	1.93	0.25
	2 <sup>nd</sup> OSA	21.9	16.8	18.39	5.10	3.51
Zigzag (-10°/10°)	1 <sup>st</sup> OSA	9.5	8.98	11.44	0.52	1.94
	2 <sup>nd</sup> OSA	15	11.18	12.58	3.82	2.42
Zigzag (20°/-20°)	1 <sup>st</sup> OSA	13.7	11.16	10.96	2.54	2.74
	2 <sup>nd</sup> OSA	14.9	16.52	15.36	1.62	0.46
Zigzag (-20°/20°)	1 <sup>st</sup> OSA	15.1	14.58	14.33	0.52	0.77
	2 <sup>nd</sup> OSA	13.3	12.6	11.67	0.70	1.63

## 6. Conclusions

In this study, hydrodynamic coefficients and parameters are defined by taking advantage of experimental data on KVLCC1 and KVLCC2 scale models by applying MMG method for maneuvering simulations. The MMG method is chosen from a selection of formerly developed mathematical methods due to its easy implementation and well agreement with actual results. In this method, the lateral hull force and yawing moment are stated in two different forms, as second order and third order polynomial. These mathematical models are checked for compliance with the free running model tests via turning circle and zigzag maneuvering simulations.

It is found that Model-1 gives better results in the starboard and port turning circle maneuvering motions for KVLCC1 and KVLCC2 hulls. Especially, at the later time of the simulation, the trajectory parameter moves away from the real value of the port turning circle simulation in both models. In zigzag ( $\pm 10^\circ/\pm 10^\circ$ ) maneuvering motions, Model-1 for KVLCC1 hull and Model-2 for KVLCC2 hull are closer to free running model test results. In zigzag ( $\pm 20^\circ/\pm 20^\circ$ ) maneuvering motions, both models give approximately the same results, which are in a good agreement with the free running model test results. It can be concluded that, the MMG model generated by the lateral hull force and yawing moment expressed by the

third order polynomial gives more realistic results when taking all of the simulations into account.

Since, all the analyses conducted at this research are based on the experiments for two ships, this is not enough to evaluate general conclusions for the maneuvering. Therefore; for future works, experiments with different scale models and different ships should be analyzed in order to gain an extended insight. Thus, a general result for maneuvering can be concluded.

## 7. Acknowledgments

For the maneuvering simulations of KVLCC1 and KVLCC2 Circular motion test results of NMRI (National Maritime Research Institute) are utilized. Furthermore; the simulations are compared with the free test results of MARIN (Maritime Research Institute Netherlands). All of these data are included in SIMMAN 2008 workshop ([www.simman2008.dk](http://www.simman2008.dk)).

## References

- [1] Zorba, Y. and Nas, S. (2016). A Study on Determination of Required Tug Force and Number of Tugs in Port Maneuvers. *Journal of ETA Maritime Science* 4(3): 215-234.
- [2] ITTC (2008). The Manoeuvring Committee Final Report and Recommendations to the 25th ITTC.
- [3] Ogawa, A., Koyama, T., and Kijima,



- K.(1977). MMG report-I, on the mathematical model of ship manoeuvring. Bull Soc Naval Archit Jpn 575:22-28 (in Japanese).
- [4] Ogawa, A. and Kasai. H (1978). On the mathematical method of manoeuvring motion of ships. Int Shipbuild Prog 25(292):306-319.
- [5] Kose,K.(1982).On a new mathematical model of maneuvering motions of a ship and its applications."International Shipbuilding Progress(29(336)): 205-220.
- [6] Yoshimura, Y. (2005). Mathematical model for manoeuvring ship motion (MMG model). Workshop on Mathematical Models for Operations involving Ship-Ship Interaction, Tokyo.
- [7] Inoue, S., Hirano, M. and Mukai, K (1979). The Nonlinear Terms of Lateral Force and Moment Acting on Ship Hull in the Case of Manoeuvring. Transactions of the WestJapan Society of Naval Architects.
- [8] Inoue, S., Hirano, M., Hirakawa, Y. and Mukai, K. (1979). The Hydrodynamic Derivative on Ship Maneuverability in Even Keel Condition. Transactions of the WestJapan Society of Naval Architects No. 57.
- [9] Simman (2008). Workshop on Verification and Validation of Ship Manoeuvring Simulation Methods. <http://www.simman2008.dk>, 2008.
- [10] Yoshimura Y., Ueno M., and Yoshiaki T. (2008). Analysis of steady hydrodynamic force components and prediction of manoeuvring ship motion with KVLCC1, KVLCC2 and KCS. Workshop on verification and validation of ship manoeuvring simulation method, Workshop Proceedings, vol 1: p. pp E80-E86.
- [11] Yoshimura, Y., Ueno, M., and Yoshiaki, T. (2008). Effects of rudder and propeller on hull force derivatives with KVLCC1 and KVLCC2. Workshop on verification and validation of ship manoeuvring simulation method, Workshop Proceedings, vol 1: p. pp E87-E90.
- [12] Japan Society of Naval Architects and Ocean Engineers. (2013). Report of Research committee on standardization of mathematical model for ship maneuvering predictions (P-29), in (in Japanese). [http://www.jasnaoe.or.jp/research/p\\_committee\\_end.html](http://www.jasnaoe.or.jp/research/p_committee_end.html)
- [13] Yasukawa, H. and Yoshimura, Y. (2015). Introduction of MMG standard method for ship maneuvering predictions. Journal of Marine Science and Technology, 20(1): 37-52.
- [14] Simman (2008). part B Benchmark Test Cases, in Workshop on verification and validation of ship manoeuvring simulation method Workshop Proceedings, Copenhagen. p. pp B2-B9.
- [15] Hoof, J. and Pieffers, J. (1988). Maneuverability of frigates in waves. Marine technology, 25(4): 262-271.
- [16] Eloot, K. (2006). Selection, experimental determination and evaluation of a mathematical model for ship manoeuvring in shallow water. Ghent University.
- [17] Fujii, H. and Tuda, T. (1961). Experimental researches on rudder performance. Journal of the Society of Naval Architects of Japan, 109: 110.
- [18] Simman (2008). part B Model Test Reports, in Workshop on verification and validation of ship manoeuvring simulation method. Workshop Proceedings, Copenhagen. p. pp B2-B9.